Establishment of Co-Culture Model of Primary Mature Adipocytes and Hepatocytes in Non-Alcoholic Fatty Liver Model Rats and its Effect on Hepatocyte Steatosis

YICHEN PENG, D. ZHENG[1], YURONG ZHANG[1], XIANGLIN CHEN AND JING WANG[1]*

Department of Integrated Traditional Chinese and Western Medicine, The Southwest Medical University, Luzhou, Sichuan 646099, [1]Hepatobiliary Department, The Affiliated Traditional Chinese Medicine Hospital of Southwest Medical University, Luzhou, Sichuan 646000, China

Peng *et al.*: Effect of Adipocyte-Hepatocyte Interaction Model in Non-Alcoholic Fatty Liver Model Rats

Non-alcoholic fatty liver, as the initial link in the development of non-alcoholic steatohepatitis, its mechanism of occurrence and development is of great significance for the treatment of clinical non-alcoholic fatty liver disease. The aim of this study was to establish a stable and reliable co-culture model of primary mature adipocytes and hepatocytes in non-alcoholic fatty liver model rats for in-depth study of adipocytes-hepatocyte interaction, revealing the pathophysiological mechanism of adipocyte effects on hepatocyte steatosis lays a pharmacological research foundation. 8 w old male Sprague-Dawley rats were randomly divided into control group and non-alcoholic fatty liver group. Control group was given normal diet and non-alcoholic fatty liver group was given high fat diet. After 6 w of continuous feeding, hematoxylin and eosin, oil red O staining and non-alcoholic fatty liver disease activity score were performed on liver tissue sections. Serum triglyceride, total cholesterol, alanine aminotransferase and aspartate aminotransferase contents were measured by kits to verify non-alcoholic fatty liver rat model which was successfully established. Rat primary mature adipocytes and hepatocytes were extracted and differentiated by collagenase *in situ* perfusion and collagenase digestion, and the co-culture system was constructed by transwell chambers. Oil red O staining and triglyceride kit were used to detect lipid accumulation in primary hepatocytes before and after co-culture; quantitative real-time polymerase chain reaction and Western blot were used to detect the expression levels of p38 mitogen-activated protein kinase, phosphorylated p38 mitogen activated protein kinases and aquaporin 9 in primary hepatocytes before and after co-culture for 48 h. The co-culture model of primary mature adipocytes and hepatocytes in non-alcoholic fatty liver model rats was successfully established and the co-culture of mature adipocytes in non-alcoholic fatty liver pathological state may be involved in hepatocyte steatosis by up-regulating the expression of aquaporin 9 through activating p38 mitogen activated protein kinase pathway.

Key words: Non-alcoholic fatty liver disease, primary mature adipocytes, primary hepatocytes, aquaporin 9, p38 mitogen-activated protein kinase

Non-Alcoholic Fatty Liver Disease (NAFLD) refers to a clinicopathologic syndrome characterized by hepatic steatosis due to exclusion of alcohol and other definite liver damage factors, and its disease spectrum includes Non-Alcoholic Fatty Liver (NAFL), Non-Alcoholic Steatohepatitis (NASH) and related cirrhosis and liver cancer[1]. In recent years, its prevalence has shown a rapid increase, parallel to the epidemic of obesity and metabolic syndrome, with a global prevalence of 24 %[2] and more than 240 million people in China currently suffer from NAFLD, accounting for more than one-fifth of NAFLD patients worldwide. According to statistics, in 2030, the number of patients in China will reach 345.8 million, becoming the country with the largest increase in the prevalence of NAFLD worldwide. However, the pathogenesis of NAFLD has not yet been elucidated and no drug has been approved by the Food and Drug Administration (FDA) for the treatment of NAFLD[3]. However, NAFL, as the initial link in the development of NASH, its mechanism of occurrence and development is of great significance for the treatment of clinical NAFLD[4].

NAFL pathogenesis is complex and hepatic steatosis is considered as a key link in NAFL progression,

while adipocyte-hepatocyte crosstalk is a potential driver of hepatic steatosis[5,6]. Studies have shown that adipocytes decompose glycerol and fatty acids more in the obese state and are taken up by hepatocytes after entering the blood resulting in Triglyceride (TG) in hepatocytes (Excessive TG) synthesis is an important pathophysiological basis for the pathogenesis of NAFL. However, direct evidence for this mechanism is lacking until now[5]. Therefore, exploring the communication mechanism and target between adipocytes and hepatocytes during the progression of NAFL has become the focus of NAFL research and the goal of prevention and treatment. How to establish an effective adipocyte-hepatocyte interaction model *in vitro* is currently a technical difficulty[7]. The aim of this study was to establish a stable and reliable co-culture model of primary mature adipocytes and hepatocytes in NAFL model rats for in-depth study of adipocytes in NAFL-hepatocyte interaction, revealing the pathophysiological mechanism of adipocyte effects on hepatocyte steatosis which lays a research foundation.

MATERIALS AND METHODS

Animals:

Adult male outbred Sprague-Dawley (SD) rats weighing 180-200 g were used in this study (Laboratory Animal Center of Southwest Medical University, Luzhou, China). 8 w old male Sprague-Dawley rats were randomly divided into control group and non-alcoholic fatty liver group. Control group was given normal diet and non-alcoholic fatty liver group was given High Fat Diet (HFD). In the control group, rats were fed (standard diet, Laboratory Animal Center of Southwest Medical University, Luzhou, China) or HFD (82 % standard diet, 10 % lard, 2 % cholesterol, 1 % bile salts, 5 % egg yolk powder, Dashuo Laboratory Animal Co. Ltd., Chengdu, China) for 6 w. All animal experimental procedures were approved by the Animal Ethics Committee of Southwest Medical University (Reference number: 20210223-024).

Chemicals:

Chemicals used in the study are collagenase I, 4-(2-Hydroxyethyl)-1-piperazineethanesulfonic acid, collagenase IV, hydrocortisone, Ethylenediaminetetracetic Acid Disodium (EDTA.2Na), Percoll dispersion, modified Oil Red O (ORO) staining kit (Solarbio, China), Dulbecco's Modified Eagle Medium (DMEM) high glucose medium, DMEM/F12 medium (Gibco, United States of America (USA)), Fetal Bovine Serum (FBS) (Pan, Germany), insulin (Invitrogen, USA); 3-Isobutyl-1-Methylxanthine (IBMX), dexamethasone (Sigma, USA); Alanine Aminotransferase (ALT), Aspartate Aminotransferase (AST), Total Cholesterol (TC) and TG kit (Nanjing Jiancheng Bioengineering Institute, China).

Main solution preparation:

Buffer solution, hepatocyte digestive juice, adipocyte digestive juice, adipocyte differentiation medium I and II were prepared to make up the main solution. Buffer solution was prepared by using Sodium bicarbonate (NaHCO$_3$), N-2-Hydroxyethylpiperazine-N'-2-Ethanesulfonic Acid (HEPES), Potassium chloride (KCl), Sodium chloride (NaCl), D-Glucose, EDTA. Further, NaHCO$_3$, HEPES, KCl, NaCl, D-Glucose, 1.2 mmol/l Calcium chloride (CaCl$_2$) and 0.03 % collagenase IV were used to prepare hepatocyte digestive juice. DMEM high glucose medium and 0.1 % collagenase I were used to prepare adipocyte digestive juice. Similarly, adipocyte differentiation medium I was prepared by using 1 μM dexamethasone, 0.5 mM IBMX and DMEM/F12 complete medium. Adipocyte differentiation medium II was also prepared using 0.5 μg/ml insulin and DMEM/F12 complete medium. All solutions were adjusted to pH 7.2-7.4 and filtered through 0.22 μm filter at 4°.

Observation of serum liver function parameters using Hematoxylin and Eosin (HE) and ORO staining:

Liver tissues were fixed in 4 % paraformaldehyde for 24 h, embedded in paraffin, sectioned and stained with HE. Frozen liver tissues in liquid nitrogen were embedded in Optimal Cutting Temperature (OCT) gel, cryosectioned and stained with ORO. Microscopically, NAFLD Activity Score (NAS) was assessed in rat liver tissue according to the guidelines of the Pathology Working Group of the NASH Clinical Research Network at the National Institutes of Health[8]. The contents of TG, TC, AST and ALT in rat serum were detected by microplate reader. The detection method was carried out in strict accordance with the kit instructions.

Establishment of co-culture system:

Isolation of NAFL primary hepatocytes and precursor adipocytes primary hepatocytes: 2 % (4 ml/kg) pentobarbital sodium in SD rats was intraperitoneally anesthetized, 75 % alcohol disinfection was performed, a "U" graphene incision was performed on the abdomen and an indwelling needle was inserted into the hepatic portal vein. The liver was perfused with buffer (40°, water bath preheated) until the intrahepatic congestion was removed, switched to hepatocyte digestive juice (40°, water bath preheated), perfused until the surface of the liver showed cracks. Then the liver was transferred to a biosafety cabinet where the liver capsule was torn open with forceps in a culture dish. The cell suspension flowed out and the cell suspension was filtered through a 70 μm filter into a 50 ml centrifuge tube, centrifuged at 1000 rpm for 3 min, the supernatant was discarded and the cells were resuspended in complete medium (10 % FBS, 1 % penicillin solution, 500 U/l insulin and 1 mM hydrocortisone, DMEM high glucose medium); 30 % Percoll cell dispersion was added to a 15 ml centrifuge tube in advance and the cell suspension was slowly added at 1500 rpm and centrifuged for 5 min, and the supernatant was transferred to another centrifuge tube to resuspend the cell pellet. Then the remaining cell suspension and Percoll cell dispersion were mixed well and after repeated centrifugation, the supernatant was discarded and resuspended, and the cell suspension was collected twice, centrifuged at 500 rpm for 3 min, the supernatant was discarded. Further, complete medium was added and trypan blue was used to identify the cell viability. After counting, the cells were seeded into the lower chamber of the transwell at a cell density of 7×10^5/ml and the medium was changed 6 h later, and then for every 2 d.

Isolation of primary precursor adipocytes: The epididymis and perirenal adipose tissue were removed to a culture dish under aseptic conditions, washed three times with cold Phosphate Buffered Saline (PBS) to remove blood clots and fibrous tissue, added with digestive juice of twice the volume of the tissue, cut the tissue into small pieces of 1 mm^3, transferred to a 50 ml centrifuge tube and shaken at 37° for digestion for 30 min in a temperature-controlled shaker until digested into chylous fluid. Then, the suspension was filtered through a 70 μm pore size cell sieve, centrifuged at 2000 rpm for

10 min. The supernatant was discarded and 10 ml of complete medium (DMEM/F12 medium, 10 % FBS) was added into the resulting cell pellet for resuspension. Inoculate the suspension in a culture dish and place in 37°, 5 % Carbon dioxide (CO_2) saturated humidity incubator for culture, and change the medium after 12 h.

Induction of differentiated primary precursor adipocytes in the transwell chamber: Induced differentiated primary precursor adipocytes are mature adipocytes. When the cells grow and fuse to 70 %-80 %, the precursor adipocytes are inoculated into the upper chamber of the transwell at 1×10^5/ml cells/well and observed to completely fuse to 100 %. Then the complete medium is replaced with differentiation medium I and differentiation medium II was replaced after 3 d of culture, and complete medium was replaced after 2 d of culture. The whole differentiation process took 7-10 d and the degree of cell differentiation was observed under a microscope regularly.

Establishment of NAFL mature fat-hepatocyte co-culture system: Adipocytes from NAFL group were seeded into transwell upper chambers and induced to differentiate with the above method for 7 d. Hepatocytes from NAFL group were seeded into transwell lower chambers at a density of 2×10^5 cells/ml for co-culture. The cells and supernatants were collected after co-culture for 48 h.

The degree of lipid accumulation assay:

Hepatocytes were washed with PBS, fixed in 4 % paraformaldehyde for 30 min. They were detected according to the instructions of the cell ORO staining kit, observed and photographed under a microscope. Cell pellets were collected, 0.2~0.3 ml of lysis solution was added and intracellular TG levels were measured according to the TG assay kit instructions.

Reverse Transcription-Polymerase Chain Reaction (RT-PCR) analysis:

Following 48 h of co-culture, total Ribonucleic Acid (RNA) was extracted from hepatocytes using a column RNA purification kit. RNA purity was assessed by calculating the A260/A280 ratio, which ranged from 1.8 to 2.0. Complementary Deoxyribonucleic Acid (cDNA) was obtained by reverse transcription and RT-PCR was performed using this cDNA as a template under the following reaction conditions, Step 1: 95° 30 s; Step 2: 95° 5 s,

55° 10 s, 72° 15 s. This step was repeated 40 times. Primers were synthesized by Sangon Biotech Co., Ltd. (Shanghai, China) (Table 1). Cycle Threshold (CT) values of target gene Aquaporin 9 (AQP9) and internal reference gene Glyceraldehyde-3-Phosphate Dehydrogenase (GAPDH) were analyzed. Relative expression levels of target genes were calculated by the $2^{-\Delta\Delta CT}$ method and statistically analyzed. The RT-PCR data collection and analysis experiment was repeated three times.

Western blotting analysis:

After 48 h of co-culture, proteins were extracted from hepatocytes with Radioimmunoprecipitation Assay (RIPA) lysate, protein concentration was detected by Bicinchoninic Acid (BCA) protein analysis kit and completely denatured after boiling in bromophenol blue sample buffer for 5 min. Equal amounts of proteins were separated by Sodium Dodecyl-Sulfate Polyacrylamide Gel Electrophoresis (SDS-PAGE) and transferred to Polyvinylidene Fluoride (PVDF) membranes which were blocked with 5 % skimmed milk for 1 h. GAPDH (Abcam, ab8245, USA), p38 Mitogen-Activated Protein Kinase (p38 MAPK) (Abcam, ab170099, USA), phosphorylated p38 MAPK (p-p38 MAPK) (Abcam, ab170099, USA), AQP9 (Abcam, aab15127, USA), primary antibodies (1:1000) were added, respectively and incubated at 4° for 12 h. The membranes were then incubated with the secondary antibodies at room temperature for 2 h. The Enhanced Chemiluminescence (ECL) kit was used for exposure development. Finally, protein bands were semiquantitatively analyzed using ImageJ. The final results were expressed as the ratio of absorbance of the target protein to that of the internal reference (protein normalization) and the experiment was repeated three times.

Statistical analysis:

All quantitative results were presented as mean±standard deviation and data analysis was performed using Statistical Package for the Social Sciences (SPSS) 24.0 and GraphPad Prism 8.0 statistical software. Comparison between two independent samples was statistically compared using the t-test and comparison between multiple groups of samples was performed using one-way Analysis of Variance (One-way ANOVA), p<0.05 was considered statistically significant.

RESULTS AND DISCUSSION

The HE staining results of rat liver tissue sections showed that in the control group, the liver tissue had normal morphology, clear structure, neatly arranged and no obvious steatosis of hepatocytes. In the NAFL group, lipid droplets of different sizes appeared in the cytoplasm of hepatocytes, which were densely scattered throughout the cytoplasm and hepatocyte steatosis was significant (fig. 1). The results of ORO staining of rat liver tissue sections showed that no significant lipid droplets were observed in hepatocytes in the control group. There were more, red lipid droplets in hepatocytes and significant steatosis in the NAFL group (fig. 2). The results of blood biochemical indicators showed that the serum TC and TG contents in the NAFL group significantly increased (p<0.05) when compared with the control group. ALT and AST contents were significantly increased (p<0.05) (fig. 3). The results of NAS scoring showed that the NAS score was significantly increased (p<0.05) in the NAFL group compared with the control group (fig. 4), with >33 % hepatic steatosis without intralobular inflammation, ballooning degeneration and fibrosis and the NAFL rat model was successfully established.

NAFL rat primary precursor adipocytes and hepatocytes were successfully isolated. Collagenase *in situ* perfusion and collagenase digestion were used to separate NAFL rat primary hepatocytes and primary precursor adipocytes, which were observed under an inverted light microscope. 6 h later, hepatocytes began to adhere and were oval in shape. 24 h later, cells were basically adhered and showed a long spindle transition in shape. 48 h later, cells were connected to each other and showed irregular paving stone, whereas preadipocytes began to adhere after 12 h, the fully adherent morphology was oval after 24 h. They gradually transitioned to long spindles after 48 h with increasing number of cells. After 72 h, cells interconnected and grew in long spindles (fig. 5A and fig. 5B).

TABLE 1: OLIGONUCLEOTIDE PRIMERS USED FOR RT-PCR

Gene	Forward primer	Reverse primer
p38 MAPK	5 '-GGACCTAAAGCCCAGCAA-3'	5 '-AAGGACGGTGCCAAGAA-3'
AQP9	5 '-AAGGACGGTGCCAAGAA-3'	5 '-ATCACGACTGCCGATGC-3'
GAPDH	5 '-CCATCCACAGTCTTCTGAGT-3'	5 '-CCTCAAGATTGTCAGCAAT-3'
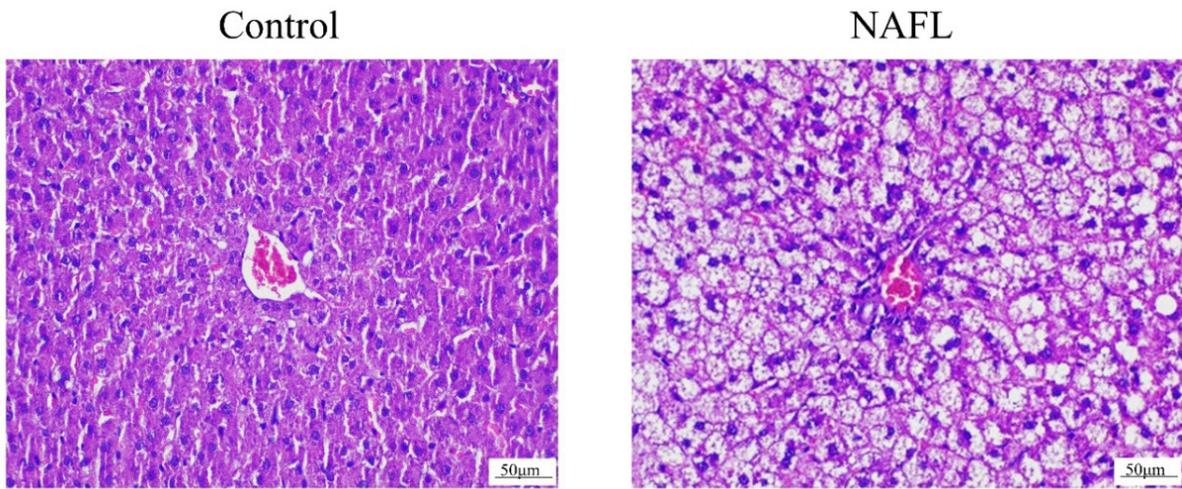
Fig. 1: The control and NAFL model rat liver tissue section observed by HE staining
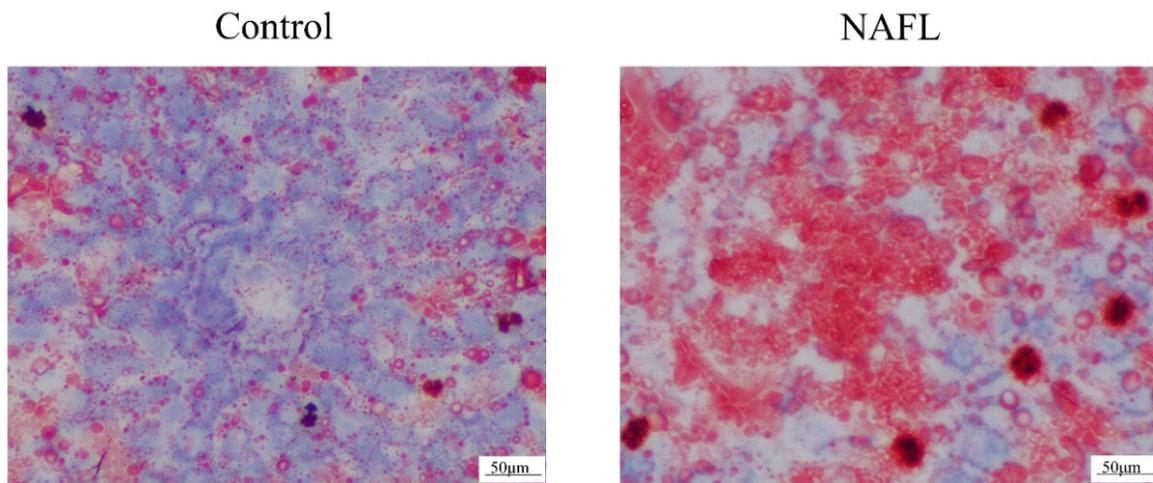
Fig. 2: The control and NAFL model rat liver tissue section observed by ORO staining
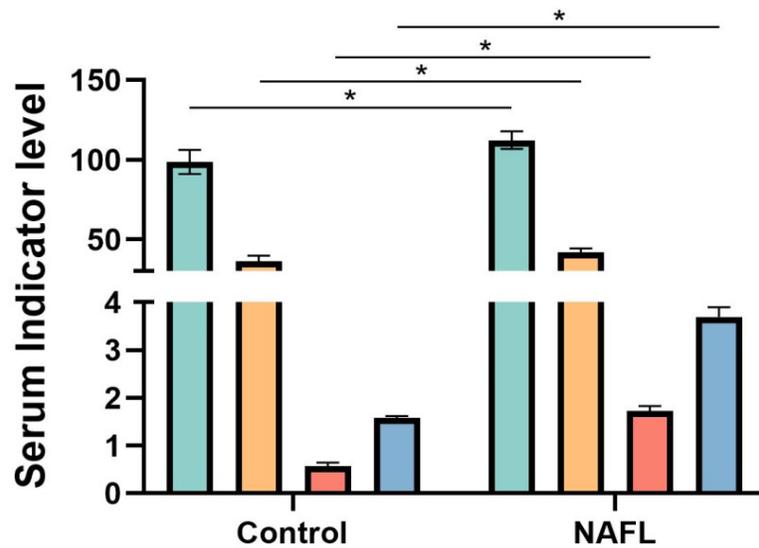
Fig. 3: Comparison of the serum lipid and liver function enzymes in rat of each group Note: *p<0.05 control *vs.* NAFL group, (▭) AST (U/l); (▭) ALT (U/l); (▭) TG (mmol/l) and (▭) TC (mmol/l)
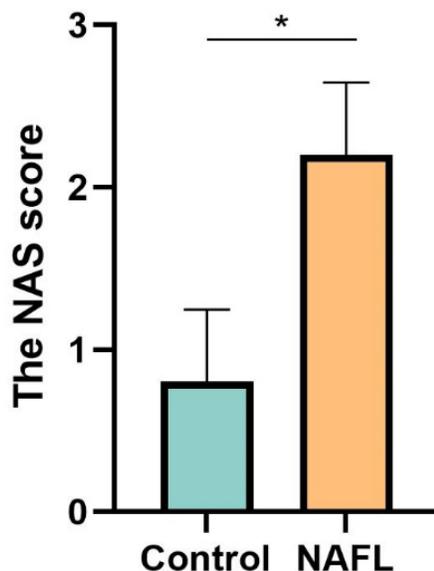
Fig. 4: The NAS of control rat and NAFL model rat liver tissue section
Note: *p<0.05 control *vs.* NAFL group

A   B
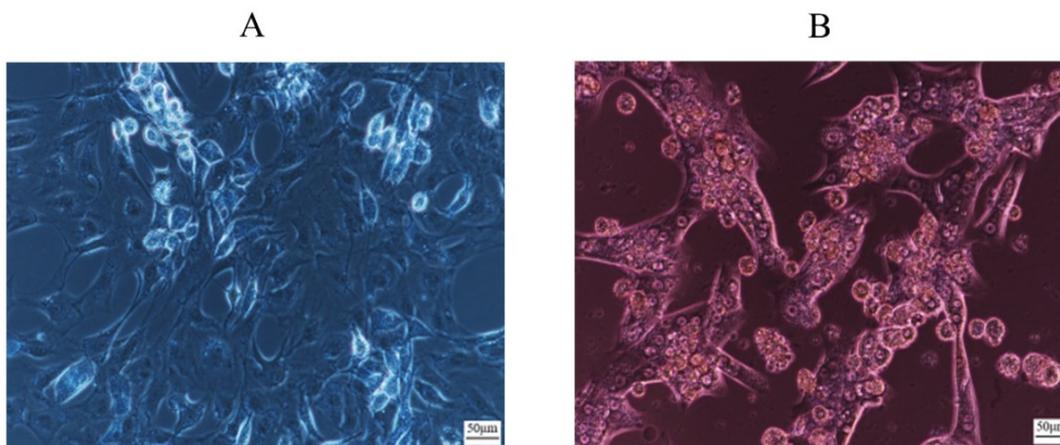
Fig. 5: (A) Primary pre-adipocytes and (B) Primary hepatocytes

Precursor adipocytes successfully differentiated into mature adipocytes. Microscopically, it was found that at 7 d after induction of precursor adipocytes, the cells were filled with a large number of radiolucent vacuoles, which were identified by ORO staining and showed ring orange lipid droplets, suggesting that precursor adipocytes had successfully differentiated into mature adipocytes (fig. 6A and fig. 6B).

Hepatocyte ORO staining and TG detection results showed that the hepatic intracellular lipid droplet density and TG content were significantly increased in the NAFL group (p<0.05) when compared with the control group. Similarly, the hepatic cellular lipid droplet density and TG content were significantly increased in the co-culture group (p<0.05) when compared with NAFL group. Additionally, the degree of steatosis was more severe (fig. 7 and fig. 8).

Compared with the control group, the NAFL group AQP9 and p38 MAPK messenger RNA (mRNA) expression levels were significantly increased (p<0.05). Compared with the NAFL group, AQP9, p38 MAPK mRNA expression was significantly upregulated in the co-culture group (p<0.05) (fig. 9).

Compared with the control group, AQP9 and p-p38 MAPK protein expression levels were significantly increased in the NAFL group (p<0.05). AQP9 and p-p38MAPK protein expression was significantly up-regulated in the co-culture group compared with the NAFL group (p<0.05) (fig. 10 and fig. 11).
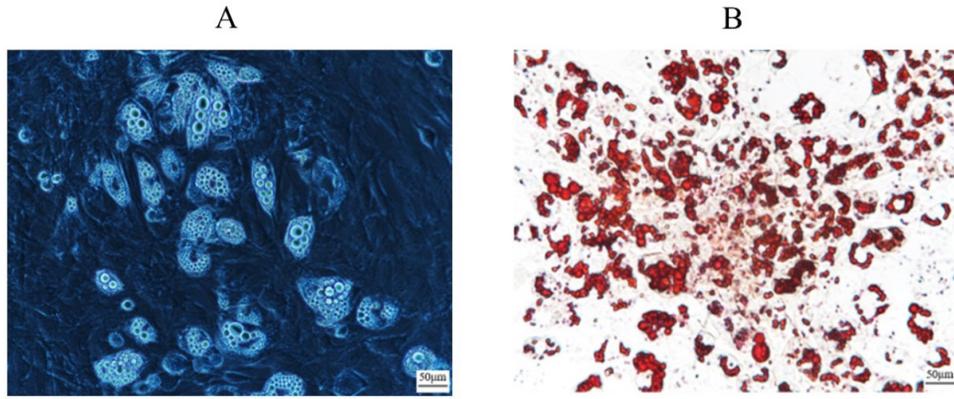
Fig. 6: Identification of mature adipocytes by (A) Inverted light microscope and (B) ORO staining
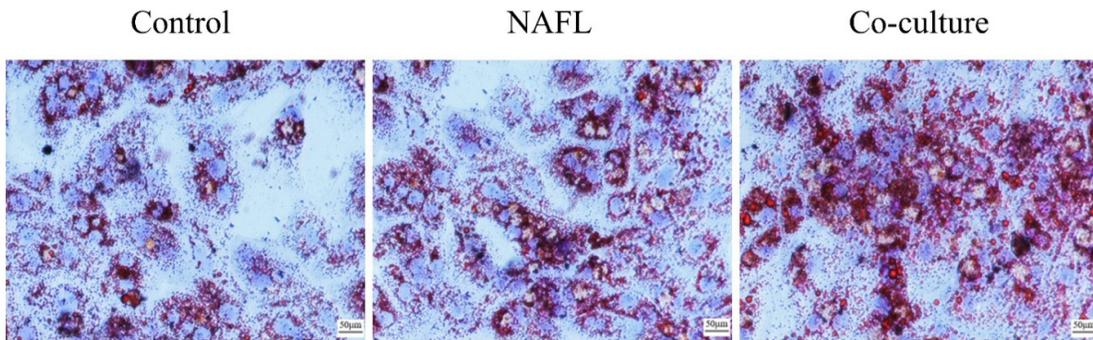
Fig. 7: Primary hepatocytes staining of control and NAFL primary hepatocytes and co-culture of primary hepatocytes observed by ORO staining
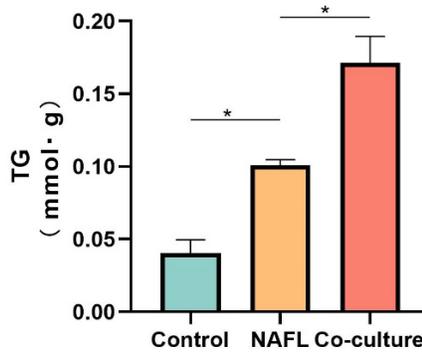
Fig. 8: The contents of TG in primary hepatocytes
Note: Data are represented as the mean±Standard Error of Mean (SEM) for five independent experiments, *p<0.05 control *vs.* NAFL group
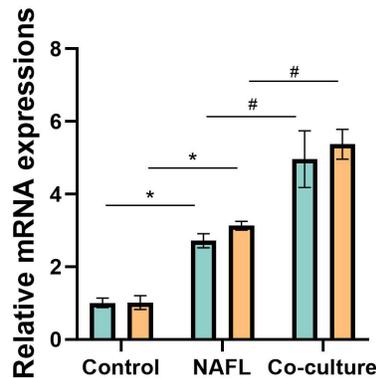
Fig. 9: The relative mRNA expressions of p38 MAPK and AQP9 in Primary hepatocytes of each group
Note: *p<0.05 control *vs.* NAFL group, #p<0.05 NAFL *vs.* co-culture group, (▭) p38 MAPK and (▭) AQP9
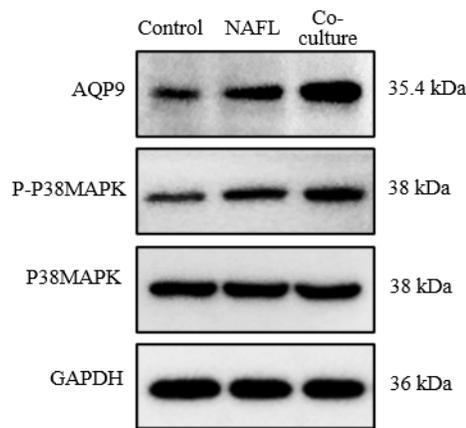
Fig. 10: Representative Western blot analysis of GAPDH, p38 MAPK, p-p38 MAPK and AQP9 in primary hepatocytes of each group
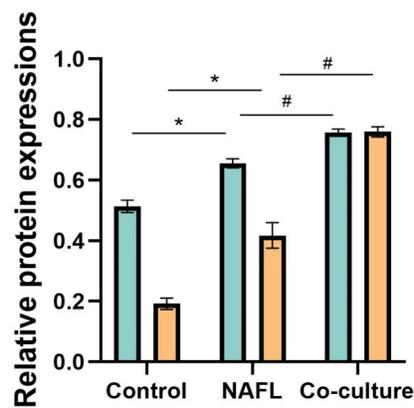
Fig. 11: Relative protein expressions of p-p38 MAPK and AQP9 in primary hepatocytes of each group
Note: *p<0.05 control *vs.* NAFL group and #p<0.05 NAFL *vs.* co-culture group, (▭) p-p38 MAPK and (▭) AQP9

The cell model has advantages of short experimental cycle such as less influencing factors and strong controllability of experimental conditions. Therefore, the establishment of NAFL adipocyte and hepatocyte co-culture model is of great significance for NAFL adipocyte and hepatocyte communication mechanism and drug testing studies[9]. At present, in the construction of co-culture system of adipocytes and hepatocytes, immortal cell lines are mostly used to study the effect of normal adipocytes on hepatocytes[10-12]. However, immortal cell lines lose their function *in vivo* due to their unlimited proliferation and immortalization characteristics, while primary cells retain their function in organs *in vivo* to a greater extent and are the cell models that best mimic the physiological and pathological conditions *in vivo*[7]. Therefore, how to establish a simple and effective co-culture model of primary adipocytes and hepatocytes in NAFL model has become a hot issue in current research.

Primary cells are difficult to extract, easy to contaminate, require higher culture conditions and have a low survival rate, while NAFL pathological conditions increase lipid droplet content in hepatocytes and precursor adipocytes, exacerbate cellular inflammation and are more fragile than normal conditions which are difficult to adhere and survive[13]. Therefore, how to stably extract primary adipocytes and hepatocytes in NAFL pathological conditions has become an urgent technical difficulty to be solved. The isolation methods of primary hepatocytes and precursor adipocytes included mechanical isolation, simple enzymatic digestion, collagenase digestion[14,15], etc. In this study, NAFL model was established by feeding SD rats with HFD and optimized in the traditional isolation method. Primary precursor adipocytes and hepatocytes of NAFL rats with large number, high purity and strong activity were successfully isolated and purified. Low speed centrifugation is mostly used for traditional primary cell isolation but due to the increased lipid droplet content in NAFL hepatocytes, cells cannot precipitate after low speed centrifugation. Further, if the centrifugation speed is too high, it is easy to lead to reduced cell viability[16]. In this study, after

exploring the centrifugation speeds such as 500 rpm, 1000 rpm and 1500 rpm, it was found that centrifugation at 1000 rpm for 3 min had the least effect on hepatocyte viability and obtained the most cell precipitation. While the traditional method uses Percoll dispersion for separation in which the cell suspension is placed on top of Percoll dispersion to obtain hepatocytes and hepatocytes can pass through Percoll dispersion with strong activity[14] by centrifugation. However, NAFL hepatocytes have few highly active cells that can pass through Percoll dispersion due to more lipid droplets and poor activity. So in this study, precipitated cells were collected on the basis of the first Percoll dispersion centrifugation. The remaining cell suspension and Percoll dispersion were mixed and centrifuged to obtain cell pellets. Finally the number of hepatocytes obtained was the highest when both the collected cell pellets were co-inoculated. This method can obtain the number of primary hepatocytes of about 7×10^5 cells/ml and the number of primary precursor adipocytes of about 1×10^5 cells/ml at one time, with a cell purity of >90 %.

Co-culture includes direct co-culture and indirect co-culture. Direct co-culture refers to the cultivation of two or more kinds of cells on the same cell container and the cells can be in direct contact with each other. Indirect co-culture refers to the separation of two types of cells in the absence of direct contact, but achieves interaction between cells in a co-culture environment[17]. Transwell chamber co-culture technique allows different types of cells to be seeded onto the bottom surface of porous membranes and inverted porous membranes, respectively, ensuring the separation of the two cells. But preserving their ability to interact through membrane pores is a commonly used experimental method for indirect co-culture[18]. Direct co-culture is able to observe the direct interaction between the two cells, but the disadvantage is that the cells cannot be separated making it difficult to explore the molecular mechanism further. Therefore, transwell chambers were selected to construct the co-culture model in this experiment. In the co-culture study, it was found that the differentiation time of precursor adipocytes was 5-10 d and the survival time of normal hepatocytes was about 7 d. While the survival time of NAFL hepatocytes was shorter than that of normal hepatocytes. After 6 d, staining with ORO, results showed that differentiation into mature adipocytes

reached the highest number at 7th d of precursor cell differentiation, while hepatocyte culture day activity was best at 3 d, when co-culture was performed.

p38 MAPK and AQP9 pathways are closely related to hepatic steatosis and play an important role in the transport of NAFL glycerol. Adipocytes secrete too many fatty acids and glycerol leading to TG accumulation in hepatocytes which is an important pathological basis for NAFL formation. By the specific mechanism of regulation of glycerol transport, the raw material for TG synthesis, between the two is not clear. AQP9, a member of the aquaporin family, is highly expressed on the hepatocyte membrane and is mainly distributed on the basement membrane side of hepatocytes adjacent to the sinusoids of the liver and is a specific channel for glycerol uptake by hepatocytes[19-21]. p38 MAPK is an evolutionarily conserved serine/threonine protein kinase that can be phosphorylated and activated by a series of extracellular stimuli, thereby transducing extracellular signals into cells and their nuclei and producing biological effects. In NAFLD, p38 MAPK drives the development of NAFL to NASH and promotes hepatic lipid accumulation[22]. Studies have shown that activation of p38 MAPK signaling pathway can up-regulate AQP9 expression on hepatocyte membranes in NAFL cell models constructed with oleic acid and AQP9 expression is directly proportional to the degree of hepatocyte steatosis. Overexpressed AQP9 can increase glycerol entering hepatocytes and administration of p38 MAPK inhibitors can reduce AQP9 expression[23]. In order to further investigate the effect of co-culture of NAFL mature adipocytes on hepatocyte steatosis, the degree of lipid deposition and the levels of p38 MAPK, p-p38 MAPK, AQP9 in hepatocytes before and after co-culture for 48 h were detected. This experiment found that the lipid deposition in hepatocytes was more severe in the co-culture group compared with the NAFL group. The mRNA and protein expression levels of p-p38 MAPK and AQP9 were significantly increased ($p < 0.05$), while the protein expression of p38MAPK was not significantly different ($p > 0.05$). This suggests that mature adipocytes are likely to contribute to hepatic steatosis by activating p38 MAPK phosphorylation and up-regulating AQP9 expression. Schematic illustration of NAFL primary steatosis induced by primary mature hepatocytes in co-culture system is shown in fig. 12.
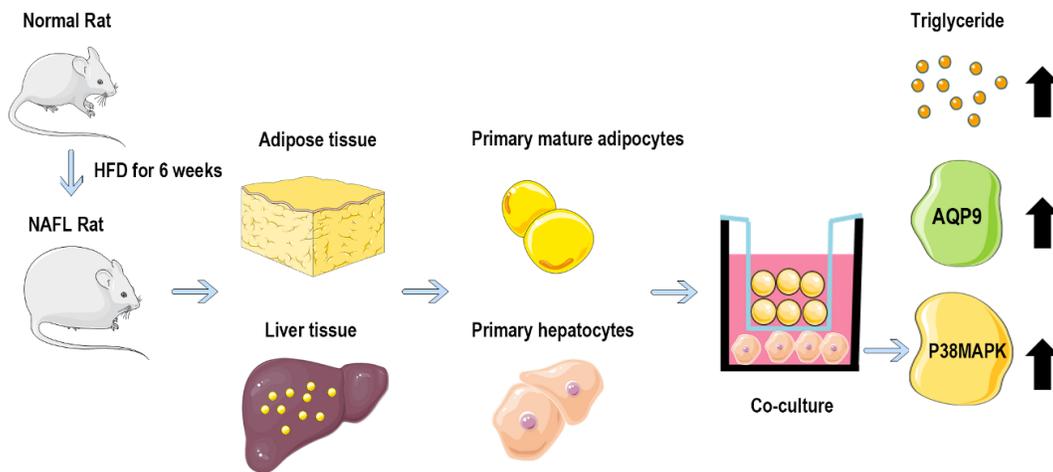
Fig. 12: Schematic illustration of NAFL primary steatosis induced by primary mature hepatocytes in co-culture system

In summary, a stable co-culture model of NAFL primary rat mature adipocytes and hepatocytes was established in this study, which provided a reliable *in vitro* model for exploring the pathophysiological mechanism and drug mechanism of NAFL. The effect of co-culture of mature adipocytes on hepatocyte steatosis was further investigated and it was found that mature adipocytes in NAFL may promote hepatocyte steatosis by affecting the expression of p38 MAPK/AQP9, laying an experimental foundation for exploring the pathogenesis of NAFL. However, the specific mechanism of p38 MAPK/AQP9 pathway regulated by mature adipocyte co-culture in hepatocytes remains to be further investigated.

Author's contributions:

Yichen Peng and Ding Zheng are co-first authors and they contributed equally to the work.

Conflict of interests:

The authors declared no conflict of interest.

REFERENCES

1. Younossi ZM. Non-alcoholic fatty liver disease-a global public health perspective. J Hepatol 2019;70(3):531-44.
2. Powell EE, Wong VW, Rinella M. Non-alcoholic fatty liver disease. Lancet 2021;397(10290):2212-24.
3. Zhou J, Zhou F, Wang W, Zhang XJ, Ji YX, Zhang P, *et al.* Epidemiological features of NAFLD from 1999 to 2018 in China. Hepatology 2020;71(5):1851-64.
4. Bence KK, Birnbaum MJ. Metabolic drivers of non-alcoholic fatty liver disease. Mol Metab 2021;50:101143.
5. Cotter TG, Rinella M. Nonalcoholic fatty liver disease 2020: The state of the disease. Gastroenterology 2020;158(7):1851-64.
6. Zhao Y, Zhao MF, Jiang S, Wu J, Liu J, Yuan XW, *et al.* Liver governs adipose remodelling *via* extracellular vesicles in response to lipid overload. Nat Commun 2020;11(1):719.
7. Liu T, Ge Y, Yuan M, Xiong Q, Zhao J. A review on cell-based models of human liver disease *in vitro*. J Biomed Eng 2021;38(1):178-84.
8. Zhing H. Guidelines of prevention and treatment for nonalcoholic fatty liver disease: A 2018 update. Chin J Hepatol 2018;26(3):195-203.
9. Khairnar R, Islam MA, Fleishman J, Kumar S. Shedding light on non-alcoholic fatty liver disease: Pathogenesis, molecular mechanisms, models, and emerging therapeutics. Life Sci 2022:121185.
10. Pelechá M, Villanueva-Bádenas E, Timor-López E, Donato MT, Tolosa L. Cell models and omics techniques for the study of nonalcoholic fatty liver disease: Focusing on stem cell-derived cell models. Antioxidants 2021;11(1):86.
11. Wang YZ, Zhang X, Li Z. Establishment of a co culture model between mature SVFs cells and Hepa1-6 cells and its effect on liver cell lipid metabolism. J Nanjing Med Univ 2022;42(5):603-9.

12. Huang TH, Li CF, Qiu LW, Liao ST, Mei ZC. Effect and mechanism of adipocyte co-culture on aquaporin-9 expression in HepG2 cells. Zhonghua Gan Zang Bing Za Zhi 2019;27(6):450-6.

13. Romualdo GR, Valente LC, Sprocatti AC, Bacil GP, de Souza IP, Rodrigues J, *et al.* Western diet-induced mouse model of non-alcoholic fatty liver disease associated with metabolic outcomes: Features of gut microbiome-liver-adipose tissue axis. Nutrition 2022;103:111836.

14. Dufau J, Shen JX, Couchet M, Barbosa TD, Mejhert N, Massier L, *et al. In vitro* and *ex vivo* models of adipocytes. Am J Physiol Cell Physiol 2021; 320(5):822-41.

15. Valdiviezo A, Brown GE, Michell AR, Trinconi CM, Bodke VV, Khetani SR, *et al.* Reanalysis of trichloroethylene and tetrachloroethylene metabolism to glutathione conjugates using human, rat, and mouse liver *in vitro* models to improve precision in risk characterization. Environ Health Perspect 2022;130(11):117009.

16. Lu XC, Han HM. Research advances in *in vitro* models for nonalcoholic fatty liver disease. J Clin Hepatol 2022;38(1):201-5.

17. Kim H, Han SH, Kook YM, Lee KM, Jin YZ, Koh WG, *et al.* A novel 3D indirect co-culture system based on a collagen hydrogel scaffold for enhancing the osteogenesis of stem cells. J Mater Chem B 2020;8(41):9481-91.

18. Hwang ST, Kang SW, Lee SJ, Lee TH, Suh W, Shim SH, *et al.* The expansion of human ES and iPS cells on porous membranes and proliferating human adipose-derived feeder cells. Biomaterials 2010;31(31):8012-21.

19. da Silva IV, Garra S, Calamita G, Soveral G. The Multifaceted role of aquaporin-9 in health and its potential as a clinical biomarker. Biomolecules 2022;12(7):897.

20. Tesse A, Grossini E, Tamma G, Brenner C, Portincasa P, Marinelli RA, *et al.* Aquaporins as targets of dietary bioactive phytocompounds. Front Mol Biosci 2018;5:30.

21. Cheng Q, Zhang J, Fang J, Ding H, Xu Y, Lu X, *et al.* Untargeted metabolomics reveals the role of AQP9 in nonalcoholic fatty liver disease in a mice model. Int J Biol Macromol 2022;219:864-75.

22. Alshehade S, Alshawsh MA, Murugaiyah V, Asif M, Alshehade O, Almoustafa H, *et al.* The role of protein kinases as key drivers of metabolic dysfunction-associated fatty liver disease progression: New insights and future directions. Life Sci 2022:120732.

23. Gu LY, Qiu LW, Chen XF, Lü L, Mei ZC. Oleic acid-induced hepatic steatosis is coupled with downregulation of aquaporin 3 and upregulation of aquaporin 9 *via* activation of p38 signaling. Horm Metab Res 2015;47(04):259-64.